

Reprinted from

2

# THE JOURNAL of the

## Acoustical Society of America

Vol. 93, No. 4, Pt. 1, April 1993

AD-A264 987



DTIC  
ELECTE  
MAY 26 1993  
S C D

### Constrained-layer damping analysis for extensional waves in infinite, fluid-loaded plates

Pieter S. Dubbelday

Naval Research Laboratory, Underwater Sound Reference Detachment, P.O. Box 508337, Orlando,  
Florida 32856-8337

pp. 1927-1935

DISTRIBUTION STATEMENT A  
Approved for public release  
Distribution Unlimited

8 5 25 060

93-11616



1105/12

REPORT DOCUMENTATION PAGE			Form Approved OMB No. 0704-0188	
Public reporting burden for this collection of information is estimated to average 1 hour per response, including the time for reviewing instructions, searching existing data sources, gathering and maintaining the data needed, and completing and reviewing the collection of information. Send comments regarding this burden estimate or any other aspect of this collection of information, including suggestions for reducing this burden, to Washington Headquarters Services, Directorate for Information Operations and Reports, 1215 Jefferson Davis Highway, Suite 1204, Arlington, VA 22202-4302, and to the Office of Management and Budget, Paperwork Reduction Project (0704-0188), Washington, DC 20503				
1. AGENCY USE ONLY (Leave blank)	2. REPORT DATE April 1993	3. REPORT TYPE AND DATES COVERED FINAL		
4. TITLE AND SUBTITLE Constrained-layer damping analysis for extensional waves in infinite, fluid-loaded plates			5. FUNDING NUMBERS PE - 61153N TA - RR011-08-42 WU - DN280-003	
6. AUTHOR(S) Pieter S. Dubbelday				
7. PERFORMING ORGANIZATION NAME(S) AND ADDRESS(ES) NAVAL RESEARCH LABORATORY UNDERWATER SOUND REFERENCE DETACHMENT P O BOX 568337 ORLANDO, FLORIDA 32856-8337			8. PERFORMING ORGANIZATION REPORT NUMBER	
9. SPONSORING/MONITORING AGENCY NAME(S) AND ADDRESS(ES) OFFICE OF NAVAL RESEARCH 800 N. QUINCY STREET ARLINGTON, VA 22217-5000			10. SPONSORING/MONITORING AGENCY REPORT NUMBER	
11. SUPPLEMENTARY NOTES				
12a. DISTRIBUTION/AVAILABILITY STATEMENT  Approved for public release; distribution unlimited.			12b. DISTRIBUTION CODE	
13. ABSTRACT (Maximum 200 words)  This study concerns the mathematical analysis of constrained-layer damping of extensional waves in plates of infinite extent, with and without fluid loading. Previous work was mostly limited to flexural waves. Some aspects of fluid loading for flexural waves may be understood by means of thin-plate theory. Therefore, a similar theory was developed for extensional waves. The description and examples presented here are based on three models: The first is an extension of Kerwin's concepts, and the third used exact elasticity theory for all three layers. It is shown that the extended Kerwin model is useful in the design of constrained-layer damping for extensional waves as well as for flexural waves.				
14. SUBJECT TERMS Constrained-layer damping      Extensional waves Flexural waves                      Fluid loading Kerwin model			15. NUMBER OF PAGES 9	
			16. PRICE CODE	
17. SECURITY CLASSIFICATION OF REPORT UNCLASSIFIED	18. SECURITY CLASSIFICATION OF THIS PAGE UNCLASSIFIED	19. SECURITY CLASSIFICATION OF ABSTRACT UNCLASSIFIED	20. LIMITATION OF ABSTRACT UL	

# Constrained-layer damping analysis for extensional waves in infinite, fluid-loaded plates

Pieter S. Dubbelday

Naval Research Laboratory, Underwater Sound Reference Detachment, P.O. Box 568337, Orlando, Florida 32856-8337

(Received 28 April 1992; revised 15 October 1992; accepted 4 December 1992)

This study concerns the mathematical analysis of constrained-layer damping of extensional waves in plates of infinite extent, with and without fluid loading. Previous work was mostly limited to flexural waves. Some aspects of fluid loading for flexural waves may be understood by means of thin-plate theory. Therefore, a similar theory was developed for extensional waves. The description and examples presented here are based on three models: The first is an extension of Kerwin's 1959 model [E. M. Kerwin, *J. Acoust. Soc. Am.* **31**, 952-962 (1959)], the second is a hybrid model in which the base plate is described by exact elasticity theory and the other two layers by Kerwin's concepts, and the third uses exact elasticity theory for all three layers. It is shown that the extended Kerwin model is useful in the design of constrained-layer damping for extensional waves as well as for flexural waves.

PACS numbers: 43.40.Dx

Accession For		
NTIS CRA&I	<input checked="" type="checkbox"/>	
DTIC TAB	<input type="checkbox"/>	
Unannounced	<input type="checkbox"/>	
Justification		
Distribution /		
Availability Codes		
	Avail and/or Special	
A-1	20	

DTIC QUALITY INSPECTED 8

## INTRODUCTION

The technique of constrained-layer damping (CLD) of acoustic waves consists of attaching a thin elastomer layer with high viscoelastic loss plus a stiff covering layer to a bar, plate, or structure. This stiff layer forces the elastomer into shear, with concomitant large loss, as compared with purely extensional damping loss in the elastomer layer without the constraining layer. Although, for a soft elastomer, the loss tangent of the shear modulus  $G$  is about the same as the loss tangent of the Young's modulus  $E$ , the energy loss in the constrained layer is of the order  $1/kh_2$  of the loss in a comparable unconstrained layer, where  $k$  is the wave number in the composite plate and  $h_2$  is the thickness of the elastomer layer.

This physical explanation of the effect is represented in a model described by E. M. Kerwin in a classical paper.<sup>1</sup> In this model the base plate is treated by thin-plate theory, thus for small values of  $kh_1$ , where  $h_1$  is the thickness of the base plate. His model gives good results within the applicable restrictions: flexural waves at low frequency in a base plate or bar with thin added layers. Extensional waves are not considered, and fluid loading is not accounted for.

It is typical for Kerwin's model that the attenuation constant  $\alpha$  is given as an explicit algebraic expression in terms of the physical and geometric parameters of the composite structure. This is an advantage in studying the influence of the various parameters on the attenuation. This author<sup>2</sup> attempted to construct an extension of Kerwin's model that retained this advantage, while relieving some of the restrictions. A short description of the extended Kerwin model is given in Appendix A, to serve as a basis for the examples in the following text. In order to include extensional waves, it was necessary to account for inertia of the constraining layer. Moreover, it became clear that the

results of the extended Kerwin model were greatly improved, when wave speeds derived from thick-plate theory were used instead of the thin-plate speeds used by Kerwin. This was true for both flexural and extensional waves.

In order to evaluate the properties of this extended Kerwin model and to check the range of its validity, a model following from exact elasticity theory for all three layers was developed. As an intermediate step, a hybrid model was constructed that contains features of both the extended Kerwin and exact models.<sup>2</sup> This model entails fewer mathematical operations than the exact model, and, as a consequence, it will produce results faster.

The two types of freely propagating waves in an infinite plate indicated by the names flexural (antisymmetric) and extensional (symmetric), collectively named Lamb waves, are mathematically distinguished by the parity of the functions representing the field variables with respect to the  $z$  coordinate, perpendicular to the faces of the plate, with the origin halfway between the faces. It follows that these two types can each occur in a pure form, without admixture of the other one, only in a situation that is strictly symmetric with respect to the  $z$  coordinate. Thus the plate should be single and homogeneous and it should be symmetrically loaded by the same type of fluid on both sides (including the unloaded case). This would appear to exclude the possibility of considering either one of these types separately when the plate is treated by constrained-layer damping on one side only and/or under one-sided fluid damping.

In studying the results from exact elasticity theory for fluid-loaded plates with constrained layer damping, when both types of waves are accounted for, it is found, though, that these two types of waves preserve their own identity even in a nonsymmetric situation. In the hybrid and fully exact models the two types are always present and, at low

values of  $kd$ , one finds two complex roots that are easily recognized as to their designation, either mostly antisymmetric or mostly symmetric. In computational practice one finds one or the other wave by starting the iterative root finder from a seed representing either type of wave, computed from thick-plate or exact theory for a single, not fluid-loaded plate. The resulting wave speed computed from the complex root is affected by the presence of the other type, but not to a large extent at low frequencies. For high frequencies it is often difficult to find an adequate seed. In experimental realizations one may create the desired type of wave by the method of excitation, for instance by means of two actuators on either side of the plate driven with opposite or equal phase. At certain values of the frequency, higher-order modes appear on the scene, determined by thickness-shear modes for flexural waves and thickness-dilatational modes for extensional waves, with some influence by the other type. At higher values of  $kd$ , the two types may be difficult to distinguish since the roots are close together and considerable accuracy was needed to separate them.

The extended Kerwin model is limited by the fact that a wave speed for a purely flexural wave or a purely extensional wave has to be entered into the computation, without accounting for the possible effect of the other type. The hybrid model uses exact elasticity theory for the base plate and, therefore, the wave speed and attenuation are both part of the root finding effort, with proper account of the other type, in asymmetric situations. It shares this aspect with the fully exact model. The fully exact model allows waves with such a large value of  $kd$  that even the elastomer layer and the constraining layer do not behave like "thin" layers. Some examples of this are given in this paper; the number of possible waves increases greatly and exceeds the range for which the notions of constrained-layer damping are practical. Except for these large values of  $kd$ , the wave speeds as computed by the fully exact model do not differ significantly from the thick-plate or exact values computed for a single, unloaded plate.

The following outline lists the three models for constrained-layer damping used in this study, with their characteristic properties.

1. Extended Kerwin model:
  - (a) Flexural or extensional waves.
  - (b) Inertia of constraining layer.
  - (c) Complex shear parameter.
  - (d) Wave speed derived from thick-plate theory for single unloaded plate.
2. Hybrid model:
  - (a) Exact elasticity theory for base plate.
  - (b) Other two layers as in extended Kerwin model.
  - (c) Simultaneous flexural and extensional waves.
  - (d) With or without fluid loading.
  - (e) Wave speed computed as part of the complex rootfinding process.
3. Exact model:
  - (a) Exact elasticity theory for all three layers.
  - (b) Simultaneous flexural and extensional waves.

- (c) With or without fluid loading.
- (d) Wave speed computed with proper account of nonsymmetric fluid-loading and influence of added layers.

In a previous study, the predictive capability of the extended Kerwin model was studied for the case of flexural waves and the effect of fluid loading.<sup>3</sup> Preliminary results of damping of extensional waves by CLD were given in short form in Ref. 4. The present paper gives an expanded account of the application of the three models to damping of extensional waves in infinite plates without and with fluid loading.

For flexural waves, valuable insight into the effect of fluid loading may be gained from thin-plate theory with fluid loading.<sup>5</sup> Therefore, a model was developed and presented in this study for extensional waves in a thin plate under fluid loading. Some results are given, based on a derivation (Appendix B) of this model. After this discussion, this paper continues with predictions from the three models for extensional waves in constrained plates without and with fluid loading. It is shown that the behavior of the attenuation as a function of frequency is strongly affected by the ratio of the extensional wave speed in the constraining layer relative to that in the base plate.

## I. THIN-PLATE THEORY FOR EXTENSIONAL WAVES IN A FLUID-LOADED PLATE

In this paper it is assumed that a straight-crested, harmonic wave propagates in the  $x$  direction parallel to the faces of the plate, with time and space dependence according to  $\exp i(kx - \omega t)$ . The complex wave number  $k$  is written as  $k = k' - i\alpha$ , where  $\alpha$  is the attenuation constant.

In Appendix B, the following dispersion relation is derived for extensional waves in a fluid-loaded plate, for thin-plate theory. This equation is given in terms of a complex variable  $\tau$ , which is related to the wave number  $k$  in the plate by  $(k_0\tau)^2 = k^2 - k_0^2$ , where  $k_0$  is the wave number in the medium, with wave speed  $c_0$ :

$$\tau^3 - \Omega\tau^2 + \tau[1 - (c_0/c_p)^2] - \Omega[1 - (c_0/c_d)^2] = 0. \quad (1)$$

Here,  $c_p$  is the thin-plate extensional wave speed in the plate, and  $c_d$  the dilatational wave speed in the plate material. A characteristic frequency  $\omega_c$  and a corresponding dimensionless frequency  $\Omega$  are introduced by  $\omega_c = (\rho_s/\rho_0)c_p^2/(c_0d)$  and  $\Omega = \omega/\omega_c$ ;  $\rho_s$  and  $\rho_0$  are the densities of the plate material and medium, respectively; and  $d$  is the half-thickness of the plate.

The characteristic frequency  $\omega_c$  for brass in water is  $1.63 \times 10^6$  rad/s, and thus for the (low-) frequency region where thin-plate theory may be applied, the nondimensional frequency  $\Omega$  is very small. As a consequence, there exists a small real root, for small  $\Omega$ , analogous to the real root for the corresponding equation for flexural waves,<sup>5</sup> namely,

$$\tau \approx \Omega \frac{1 - (c_0/c_d)^2}{1 - (c_0/c_p)^2}. \quad (2)$$

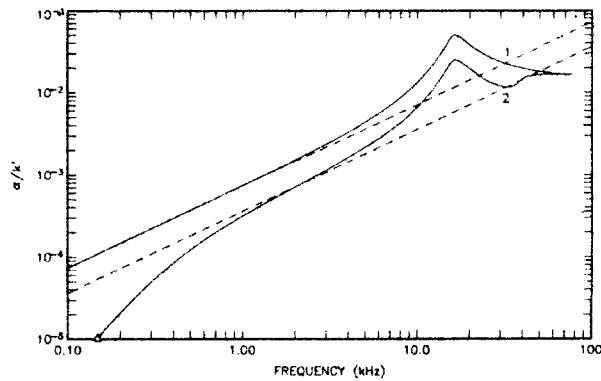


FIG. 1. Attenuation factor  $\alpha$  relative to the real part of the wave number  $k'$  as a function of frequency  $f$ , for a single 10-cm-thick brass plate, loaded by water. Solid curves are computed according to exact elasticity theory, dashed curves according to thin plate theory. Curves 1 are for water on both sides, curves 2 for water on one side.

By division one determines the quadratic equation for the two remaining complex conjugate roots,

$$\tau^2 + a\tau + b = 0, \quad (3)$$

where

$$a = \Omega \frac{(c_0/c_p)^2 - (c_0/c_d)^2}{1 - (c_0/c_p)^2} \quad \text{and} \quad b = 1 - \left(\frac{c_0}{c_p}\right)^2.$$

One of these roots leads to a wave number with positive attenuation constant  $\alpha$ . (The other root, with negative attenuation constant, has no physical significance.)

For small values of  $\Omega$  the phase speed is very close to  $c_p$  and the attenuation  $\alpha$  relative to the real part of the wave number  $k'$  is approximated by

$$\frac{\alpha}{k'} \approx 0.5 \frac{\rho_0 \omega d (c_0/c_p)^2 - (c_0/c_d)^2}{\rho_s c_0 [(1 - (c_0/c_p)^2)]^{1/2}}. \quad (4)$$

In Fig. 1 a comparison is shown of the relative attenuation  $\alpha/k'$  for a single fluid-loaded plate, according to thin-plate theory (dashed curves) and to exact elasticity theory (solid curves). The plate is 10-cm-thick brass. The curves indicated by 1 correspond to two-sided loading by water. One may observe that the agreement between the two models is excellent, except at higher frequencies. Although the boundary conditions for extensional waves cannot be satisfied for one-sided fluid loading without additional flexural waves, one might adapt the thin-plate theory by taking half the value of the total fluid stress term  $q^f$  (equal to the sum of the stresses on the two faces of the plate), as given for two-sided loading, and carrying this value for  $q^f$  through the analysis. The results are shown in Fig. 1 by the curves marked 2. It shows that the attenuation for one-sided fluid-loading thus computed does not compare well with the exact-elasticity result.

One may observe in Fig. 1 that the two solid curves marked 1 and 2 differ by a factor of two over most of the frequency range. At the high-frequency end the two curves merge, thus indicating that the radiation in the plate loaded on one side is the same as for loading on both sides.

TABLE I. Material parameters and derived quantities.

	A. Brass	B. Aluminum	C. Silver
Young's modulus $E$	104 GPa	71 GPa	78 GPa
Poisson's ratio $\nu$	0.37	0.33	0.37
Density $\rho$	8500 kg/m <sup>3</sup>	2700 kg/m <sup>3</sup>	10 500 kg/m <sup>3</sup>
Shear wave speed $c_s$	2113 m/s	3149 m/s	1647 m/s
Extensional wave speed (thin)	$c_p$ 3765 m/s	5462 m/s	2933 m/s
Characteristic frequency, for 10-cm plate	$\omega_c$ 1.63 Mrad/s	1.09 Mrad/s	1.22 Mrad/s
Dim. less freq. $k_s d$	1.49	1.00	1.07
$k_s = 2\pi f/c_s$ $d = 0.05$ m; $f = 10$ kHz			
Viscoelastic layer (hypothetical)			
Real part of shear modulus		$G_2 = 10$ MPa	
Loss tangent of shear modulus		$\beta = 1$	
Bulk modulus		$K_2 = 1$ GPa	
Fluid, water			
Density		$\rho_0 = 998$ kg/m <sup>3</sup>	
Wave speed		$c_0 = 1481$ m/s	

It appears that for extensional waves the wave energy moves to the side of the fluid, opposite to the behavior for flexural waves.<sup>3</sup>

There is a characteristic difference between the influence of fluid loading in flexural versus extensional waves. The phase speed of flexural waves increases with frequency from zero to the Rayleigh wave speed. Thus, for most cases, there will be a frequency, named the coincidence frequency,<sup>5</sup> for which the flexural wave speed is equal to the wave speed in the fluid. This plays an important role in the occurrence of radiation. In contrast, for most combinations of plate material and fluid, the extensional wave speed will be larger than the wave speed in the medium for all frequencies.

## II. DAMPING OF EXTENSIONAL WAVES

In order to show the relative merits of the three models described before, various combinations of material and geometric parameters are chosen. The generality of the results would be more clearly revealed by expressing all parameters in dimensionless form, including the abscissa of the curves shown. The representation of parameters and results in dimensional form, though, offers a more concrete feeling for the phenomena. It is remarkable that dimensionless representation of wave speeds or wave numbers for Lamb waves in unloaded plates is very similar for different materials; the graphs depend only slightly on Poisson's ratio (see Ref. 6). A useful expression for the frequency in dimensionless form is the product  $k_s d$ , where  $k_s$  is the wave number for shear waves in the plate material and  $d$  the half-thickness of the plate. To appreciate its relationship to the frequency, the value of  $k_s d$  for the various materials and a plate of 0.1-m thickness is shown in Table I. The wave speeds in the hybrid and fully exact models are in each case computed from the complex wave number found by the complex root finder. The wave speeds are only

slightly influenced by the added layers and by fluid loading at small values of  $kd$ . Only at large values of  $kd$  do sizable deviations occur (as one seen in Fig. 8). At these large frequencies the situation becomes complicated and is dependent on the given combination of materials and thicknesses.

The study of the algebraic expression for the extended Kerwin model shows some peculiar structures, as is discussed below. These same features show up in the hybrid and fully exact models. In addition, these two latter models show features at high frequency that are not contained in the extended Kerwin model. Insofar as a physical interpretation is found (e.g. concerning Fig. 8), these phenomena are considered to be general in nature, and not a product of the chosen combination of specific parameters.

A major point in the development of the extended Kerwin model is the introduction of inertia of the constraining layer. This corresponds to the appearance of the factor  $[1 - (c/c_3)^2]$  in the right-hand side of Eq. (A1) of Appendix A, where  $c_3$  is the extensional wave speed in the constraining layer, at low frequency given by the thin-plate extensional speed, and  $c$  is the pertinent wave speed in the base plate. For flexural waves at low frequency it is generally true that  $c \ll c_3$ , and this factor is then close to one. For extensional waves at low frequency,  $c$  is equal to  $c_p$ , the thin-plate extensional wave speed of the base plate material. Thus it follows that, at low frequency, extensional waves are not damped by the constrained-layer technique if the constraining plate is made of the same material as the base plate, since then this factor reduces to zero. Further, the maximum value of the third factor in the right-hand side of Eq. (A1), given by Eq. (A3), is dependent on the algebraic sign of  $[1 - (c/c_3)^2]$ . It will be shown that this leads to a considerable increase of the maximum damping for extensional waves, if the extensional wave speed in the constraining layer is less than that in the base plate, other factors being equal.

In the first set of examples, the materials and layer thicknesses are identical to those in the previous work on flexural waves.<sup>2,3</sup> There the base plate was chosen to be brass, the elastomer layer was given hypothetical values, independent of frequency, and the constraining layer was aluminum. The physical parameters of these and other materials used in the following examples are given in Table I. The thickness of the base plate is 10 cm in all cases. Equation (A2) of Appendix A shows that the maximum damping is found for a given value of the real part of the shear parameter  $g'$ , depending on the wave speeds in base plate and constraining layer and the loss tangent of the shear modulus of the elastomer. According to the definition of  $g$  this maximum can be moved to a desired frequency by the choice of the product of the thicknesses of elastomer and constraining layers  $h_2 h_3$ . The second factor in the right-hand side of Eq. (A1) shows that the damping increases with increasing thickness  $h_3$ . Of course, there are practical limitations to a large  $h_3$ , apart from the restriction to a thin constraining layer, implicit in the model. The ratio of the thickness of the constraining layer  $h_3$  to that of the elastomer layer  $h_2$  is set equal to 2 (arbitrarily). The param-

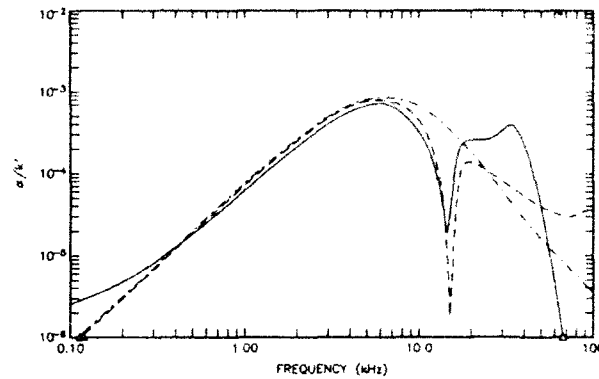


FIG. 2. Attenuation factor  $\alpha$  relative to the real part of the wave number  $k'$  as a function of frequency  $f$ , for a constrained plate in vacuum. The physical parameters for the three layers are given in Table I. The base plate is 10-cm brass, the elastomer layer is 1.24 mm thick, the constraining layer is 2.48-mm aluminum. The solid curve is computed according to the exact model, the dashed curve according to the hybrid model, and the dotted-dashed curve according to the extended Kerwin model.

eters were chosen such that the maximum damping was near 1000 Hz, for flexural waves. Then  $h_2 = 1.24$  mm, and  $h_3 = 2.48$  mm. This set of geometric parameters is also used for the first set of extensional wave examples, denoted as case A. To demonstrate the application of the extended Kerwin model, the next case, B, employs thicknesses of the constraining and elastomer layers that produce maximum damping of extensional waves near 1000 Hz. Again demanding a ratio of 2, one finds that  $h_2 = 7.75$  mm and  $h_3 = 15.5$  mm.

### III. MAXIMUM DAMPING AT 6200 HZ (CASE A)

#### A. Constrained plate in vacuum, aluminum constraining layer

In Fig. 2, a threefold comparison is shown for the relative attenuation constant  $\alpha/k'$  for extensional waves propagating in a constrained plate, without fluid loading, for the three models. The physical parameters for the three layers are given in Table I. They are the same as those for the flexural wave examples in Ref. 3. The thicknesses of the elastomer and constraining layers were chosen such that the maximum relative attenuation for flexural waves was near 1000 Hz, while  $h_3 = 2h_2$ .

One sees that the maximum relative attenuation for extensional waves has shifted to about 6200 Hz. This is due, first, to the fact that the numerator in the right-hand side of Eq. (A2) is smaller for extensional waves than for flexural waves. Second, according to the definition for the shear parameter  $g$  in Appendix A, it is inversely proportional to the square of the wave number  $k'$ . In order to maintain a given value for  $g$  at the larger extensional wave speed, as compared with the flexural wave speed, the frequency will have to be accordingly higher.

The sharp dip in attenuation near 15 kHz is due to an "equivoluminal mode,"<sup>7</sup> whereby the tangential velocity component at the faces of the plate is zero; thus no shear exists in the elastomer layer, and thus no viscoelastic damping. Of course, this feature does not show up in the

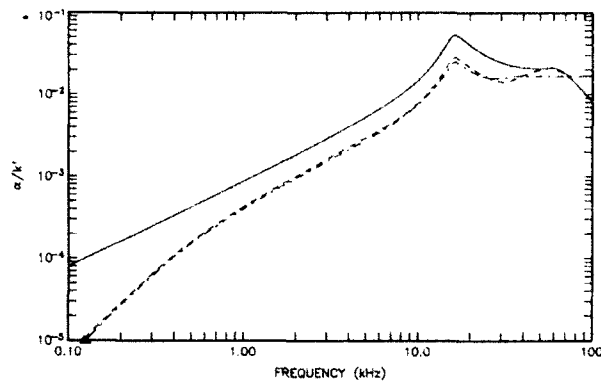


FIG. 3. Attenuation factor  $\alpha$  relative to the real part of the wave number  $k'$  as a function of frequency  $f$ , for a constrained plate loaded by water, according to exact elasticity theory. The physical parameters for the three layers are given in Table I. The base plate is 10-cm brass, the elastomer layer is 1.24 mm thick, the constraining layer is 2.48-mm aluminum. Solid curve: water on both sides; dashed curve: water on constrained side; dotted-dashed curve: water on opposite side.

extended Kerwin model, which does not account for any structure of the wave fields in the base plate. Apart from this phenomenon, there appears to be reasonable agreement between the results of the three models in the middle-frequency range.

### B. Fluid-loaded constrained plate, aluminum constraining layer

In Fig. 3, a comparison is shown for the relative attenuation constant  $\alpha/k'$  as a function of frequency for a constrained plate loaded by water on both sides, on the side of the constraining layer, and on the opposite side, computed by exact elasticity theory. One sees that, for a large frequency range, the curves are practically identical to those of Fig. 1. The viscoelastic damping, which is much smaller than the radiation damping, is apparently just added to the latter, without much influence of the fluid on the composite plate. Only at the high-frequency end is there a structure different from the one in Fig. 1, which is apparently due to this interaction: the two curves for loading on both sides and on the constrained side merge and show a decrease in attenuation not observed in Fig. 1.

### C. Constrained plate in vacuum, silver constraining layer

In Ref. 8 it was pointed out that the expression for the viscoelastic damping of extensional waves predicts increased damping when the extensional wave speed in the constraining layer is less than that in the base plate. The condition for optimum damping, Appendix A, Eq. (A2) appears in this case as

$$g' = [(c/c_3)^2 - 1] / (1 + \beta^2)^{1/2}; \quad (5)$$

the denominator of Eq. (A3) becomes small, due to the term  $2 \operatorname{sgn}[1 - (c/c_3)^2]$ . This amounts to a relaxation type of interaction between the base plate and the constraining layer, with strong attenuation.

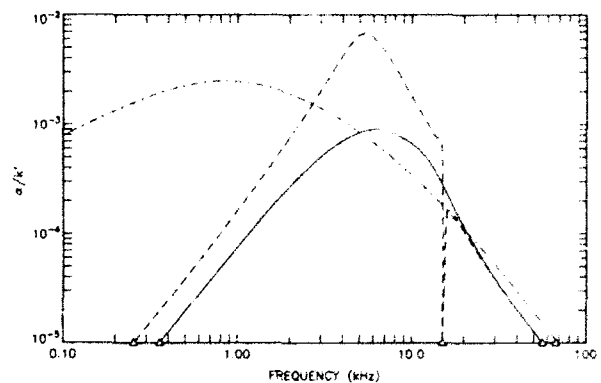


FIG. 4. Attenuation factor  $\alpha$  relative to the real part of the wave number  $k'$  as a function of frequency  $f$ , for a constrained plate in vacuum, according to the extended Kerwin model. The physical parameters for the three layers are given in Table I. The base plate is 10-cm brass, the elastomer layer is 1.24 mm thick. Solid curve: extensional wave, constraining layer 2.48-mm aluminum; dashed curve: extensional wave, constraining layer is 2.48-mm silver; dotted-dashed curve: flexural wave, constraining layer is 2.48-mm aluminum.

As an example, the aluminum constraining layer is replaced with a silver layer of the same thickness. It is not claimed that silver is a good constraining-layer material in practice, but it is used to provide a demonstration by means of an existing material. Silver was chosen because it has an extensional wave speed (2933 m/s) relative to that of brass (3765 m/s) that is about the inverse of the extensional wave speed of aluminum (5462 m/s), relative to that of brass. In Fig. 4 a comparison is given for three cases, based on the extended Kerwin model. In all cases the thickness of the brass base plate is 10 cm. The solid line gives the attenuation when the constraining layer is 2.48-mm-thick aluminum. This may be compared with the attenuation for flexural waves for the same system, the dotted-dashed curve. When the constraining layer is 2.48-mm-thick silver, the maximum relative attenuation increases by a factor of about 7, or 17 dB. This is due to the ratio of the maximum of the third factor in Eq. (A1), given in Eq. (A3), for the two cases:  $\operatorname{sgn}[1 - (c/c_3)^2]$  is minus and plus, respectively. The second factor in Eq. (A1) is practically the same in the two cases. The sharp dip in the dashed curve is a consequence of the variation of the extensional wave speed of the base plate with frequency, in thick-plate or exact theory. Considering the third factor of Eq. (A1) as a function of  $c/c_3$ , it has a maximum for  $c/c_3 = [1 + g'(1 + \beta^2)]^{1/2}$  and a minimum (zero) for  $c/c_3 = 1$ . These extrema are closely spaced in frequency for small  $g'$ , as is the case in the present example (see also Appendix A).

Figure 5 shows the comparison for the aluminum-silver combination between the extended Kerwin, hybrid, and exact models. One sees that up to about 10 kHz the agreement is quite good. Above that frequency, the exact model shows a peculiar structure that has not been explained physically. The dip apparent in the Kerwin curve is masked in the hybrid curve by the wider equivoluminal dip, which occurs at about the same frequency.

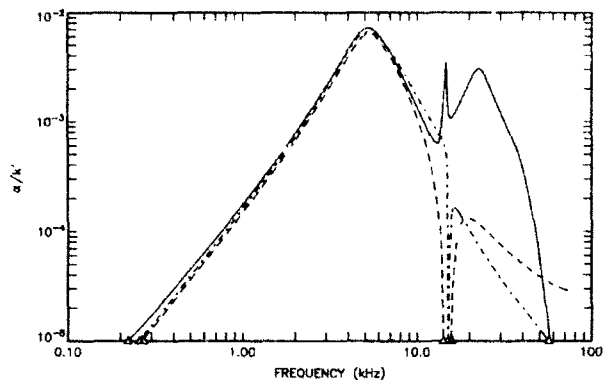


FIG. 5. Attenuation factor  $\alpha$  relative to the real part of the wave number  $k'$  as a function of frequency  $f$ , for a constrained plate in vacuum. The physical parameters for the three layers are given in Table I. The base plate is 10-cm brass, the elastomer layer is 1.24 mm thick, the constraining layer is 2.48-mm silver. Solid curve: exact elasticity theory, dashed curve: hybrid model, dotted-dashed curve: extended Kerwin model.

#### IV. MAXIMUM DAMPING AT 1000 HZ (CASE B)

##### A. Constrained plate in vacuum

In the following examples, the thickness of constraining and elastomer layers are adjusted such that the maximum viscoelastic damping for extensional waves is near 1000 Hz. In Fig. 6, the solid curve shows the result for the relative attenuation when the constraining plate is aluminum, according to the Kerwin model. As before, for case A, if one replaces the aluminum cover plate with a silver one, a higher attenuation is reached. The dashed curve shows the result from the extended Kerwin model, for a silver constraining layer. The hybrid model gives the dotted-dashed curve in Fig. 6 for this case, which is slightly different from the extended Kerwin model result.

The corresponding curve computed by the exact theory displays quite a different picture above 4000 Hz, as the solid curve in Fig. 7 shows, in comparison with the dashed curve for the hybrid model. The first large peak near 5 kHz

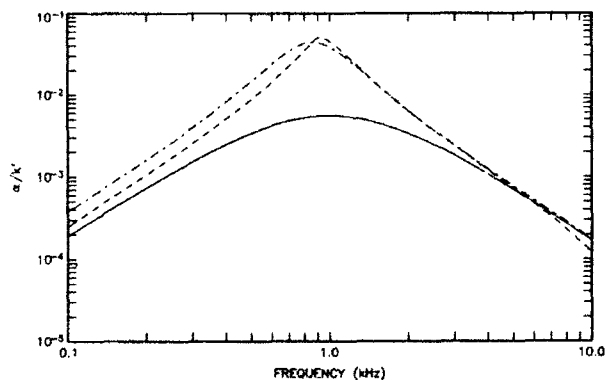


FIG. 6. Attenuation factor  $\alpha$  relative to the real part of the wave number  $k'$  as a function of frequency  $f$ , for a constrained plate in vacuum. The physical parameters for the three layers are given in Table I. The base plate is 10-cm brass, the elastomer layer is 7.75 mm thick. Solid curve: extended Kerwin model, constraining layer 15.5-mm aluminum; dashed curve: hybrid model, constraining layer 15.5-mm silver; dotted-dashed curve: extended Kerwin model, constraining layer 15.5-mm silver.

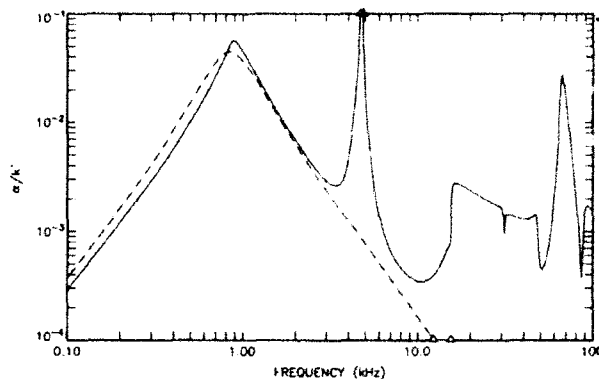


FIG. 7. Attenuation factor  $\alpha$  relative to the real part of the wave number  $k'$  as a function of frequency  $f$ , for a constrained plate in vacuum. The physical parameters for the three layers are given in Table I. The base plate is 10-cm brass, the elastomer layer is 7.75 mm thick, the constraining layer is 15.5-mm silver. Solid curve: exact model; dashed curve: hybrid model.

corresponds to the first narrow peak in Fig. 5. The character of the structure above 10 kHz may be made comprehensible by inspection of Fig. 8, where the wave speed is given as a function of frequency, together with the extensional wave speeds for a 10-cm brass plate and a 12.6-mm silver plate. The wave speed in the constrained plate appears to mostly follow the brass curve up to the point of intersection of brass and silver curves. From there it follows the silver wave speed for a while, and then meanders in the space between the silver and brass curves, to rejoin the brass curve at the next point of intersection. Fragments of other branches (not shown) were found, but were not followed throughout the frequency range.

##### B. Fluid-loaded constrained plate

Figure 9 depicts the results according to the hybrid model for a constrained plate loaded by water on both sides, on the side of the constraining layer, and on the

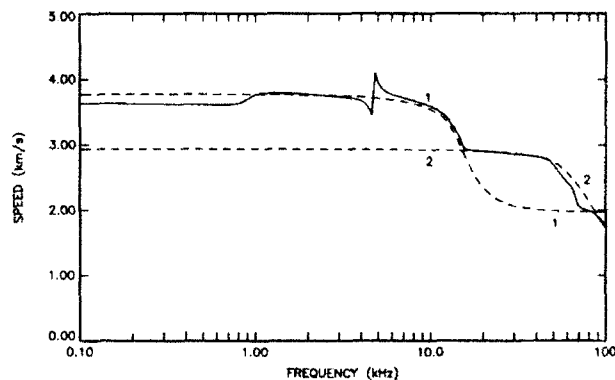


FIG. 8. Phase speed  $c$  as a function of frequency  $f$  for a constrained plate in vacuum, compared with phase speeds for single plates, according to exact elasticity theory. The physical parameters for the three layers are given in Table I. Solid curve: base plate is 10-cm brass, the elastomer layer is 7.75 mm thick, the constraining layer is 15.5-mm silver; dashed curve #1: 10-cm thick brass plate in vacuum; dashed curve #2: 15.5-mm-thick silver plate in vacuum.

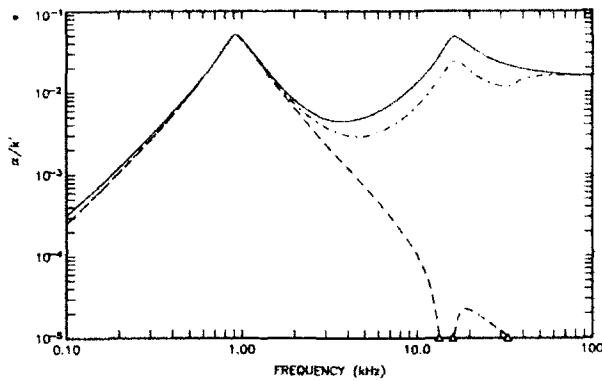


FIG. 9. Attenuation factor  $\alpha$  relative to the real part of the wave number  $k'$  as a function of frequency  $f$ , for a constrained plate, according to the hybrid model. The physical parameters for the three layers are given in Table I. The base plate is 10-cm brass, the elastomer layer is 7.75 mm thick, the constraining layer is 15.5-mm silver. Solid curve: water on both sides; short- and long-dashed curve: water on side of constraining layer or opposite side (these cases are indistinguishable at this scale); dashed curve: no fluid loading.

opposite side. The latter two cases are indistinguishable at the scale of the figure. The dashed curve is for an unloaded composite plate. One may clearly distinguish a lower frequency range, where viscoelastic damping dominates, and an upper range, where radiation is the main damping mechanism, and where the curves look very similar to those of Fig. 1 for a single plate. The exact model for fluid loading on both faces shows a slightly different picture (Fig. 10): a third peak appears between the two peaks of Fig. 9, obviously related to the high peak identified in Fig. 7 near 5 kHz, and thus indicative of viscoelastic damping. It is unexpected, though, that the radiation peak near 20 kHz is lower than predicted by the hybrid model (dashed curve), which coincides at high frequency with the radiation damping by a single plate (dotted-dashed curve). This would seem to be another manifestation of interaction of radiation and viscoelastic damping.

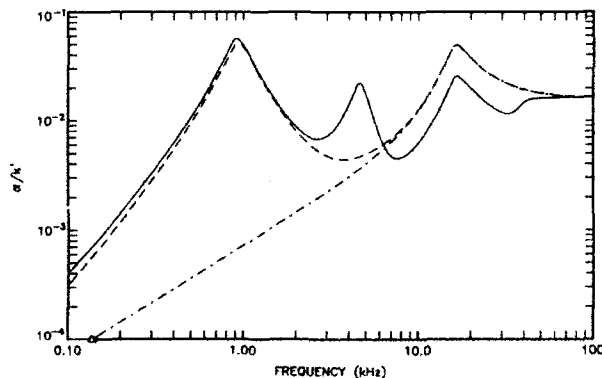


FIG. 10. Attenuation factor  $\alpha$  relative to the real part of the wave number  $k'$  as a function of frequency  $f$ , plate loaded by water on both sides. The physical parameters for the three layers are given in Table I. The base plate is 10-cm brass. Solid curve (exact model) and dashed curve (hybrid model) for constrained layer, with 7.75-mm-thick elastomer layer and 15.5-mm silver constraining layer; dotted-dashed curve (exact model) for single plate.

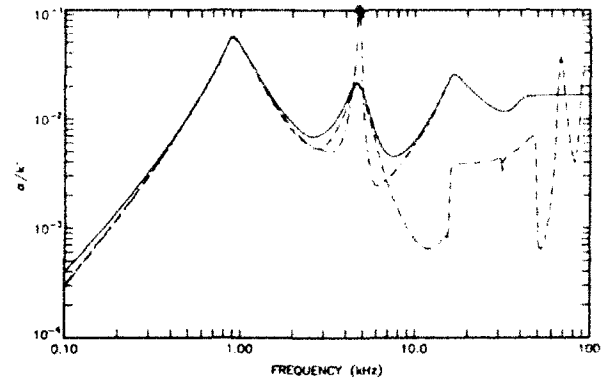


FIG. 11. Attenuation factor  $\alpha$  relative to the real part of the wave number  $k'$  as a function of frequency  $f$ , for a constrained plate, according to the exact model. The physical parameters for the three layers are given in Table I. The base plate is 10-cm brass, the elastomer layer is 7.75 mm thick, the constraining layer is 15.5-mm silver. Solid curve: both sides loaded by water; dashed curve: side of constraining layer loaded by water; dotted-dashed curve: opposite side loaded by water.

In Fig. 11 the effect of fluid loading is demonstrated, for fluid loading on both sides, on the side of the constraining layer, and on the opposite side, as computed by the exact model. The result for the fluid loading on the side of the constraining layer is strikingly different from the two other fluid-loading modes; it appears to reflect the behavior for the unloaded plate of Fig. 7, with an increasing radiation contribution added for increasing frequency. One is inclined to interpret this as an effect of the motion in the plate being drawn, at high frequencies, to the side of the fluid loading the plate: if the fluid is at the constraining-layer side, both viscoelastic and radiation damping effects are visible. Thus, the situation is, in a sense, complementary to that for flexural waves, but caution is required, since the structure of the curves is more complicated for extensional waves.

## V. SUMMARY AND CONCLUSIONS

A thin-plate theory for extensional waves in a fluid-loaded plate was presented that gives good agreement with the exact theory in the case of loading by water on both sides.

The damping of extensional waves in infinite constrained plates without and with fluid loading was analyzed by three models: the extended Kerwin model, the hybrid model, and the exact model.

The extended Kerwin model is of importance for designing constrained-layer damping applications with specific properties, since it expresses the attenuation constant explicitly in terms of physical and geometric parameters. It is limited to cases where the elastomer and constraining layer are thin relative to the base plate, and it does not account for fluid loading.

The hybrid model is useful for predicting the effect of fluid loading, and is reliable for most frequency ranges of

practical importance. It requires fewer operations than the exact model. Both the hybrid and the exact model imply finding the complex roots of an equation formed by setting the determinant value of a matrix equal to zero. For the hybrid model, this matrix has order  $4 \times 4$ ,  $5 \times 5$ , or  $6 \times 6$ , depending on whether the constrained plate is in vacuum, loaded by fluid on one side, or two sides, respectively. For the exact model the order is  $12 \times 12$ ,  $13 \times 13$ , or  $14 \times 14$ .

The exact model is the best model within the limitations of linear structural acoustics. It is recommended as a backup to the two other models, especially in situations that differ from the traditional CLD conditions of metallic plates with thin added layers at modest frequency-thickness products.

The constrained layer damping of extensional waves displays a few features not applicable to the damping of flexural waves.

(i) It is necessary to use a constraining layer of a material different from the base plate material.

(ii) There is a peculiar relaxation-type behavior of the damping when the extensional wave speed in the constraining layer is less than that in the base plate.

(iii) For one-sided fluid loading, there are indications that the wave amplitude on the loaded side increases with increasing frequency, contrary to the case of flexural waves, where the wave energy moves to the face opposite to the loaded face.

#### ACKNOWLEDGMENT

This study was supported by the Office of Naval Research.

#### APPENDIX A: EXTENDED KERWIN MODEL

In Ref. 2 the following expression was proposed as an extension of the Kerwin model:

$$\frac{\alpha}{k'} = (r\beta) \frac{E_3^* h_3}{E_1^* h_1} \frac{g' [1 - (c/c_3)^2]^2}{[1 - (c/c_3)^2 + g']^2 + \beta^2 g'^2}, \quad (\text{A1})$$

where  $\alpha/k'$  = the attenuation constant  $\alpha$  relative to the real part of the wave number  $k'$ ;  $\beta$  = the loss tangent of the elastic shear modulus;  $c$  = the speed of flexural or extensional waves from the thick-plate or exact theories;  $c_3$  = the extensional wave speed in layer 3;  $E_{1,3}^*$  = the Young's modulus of layers 1 and 3;  $E^* = E/(1-\nu^2)$ , where  $\nu$  is the Poisson ratio;  $g$  = the shear parameter,  $g = G_2/(k'^2 E_3^* h_2 h_3)$ , and  $g = g'(1+i\beta)$ ;  $G_2$  = the complex shear modulus of the elastomer,  $G_2 = G_2'(1+i\beta)$ ; and  $h_i$  = the thickness of layer  $i$ ,  $i=1,2,3$ ;  $r=3/4$  for flexural waves and  $1/2$  for extensional waves.

The third factor, considered as a function of the real part of the shear parameter  $g'$ , has a maximum for

$$g' = |1 - (c/c_3)^2| / (1 + \beta^2)^{1/2}; \quad (\text{A2})$$

the maximum value of this factor is

$$\frac{|1 - (c/c_3)^2|}{2(1 + \beta^2)^{1/2} + 2 \operatorname{sgn}[1 - (c/c_3)^2]}. \quad (\text{A3})$$

For high frequency, the extensional wave speed  $c$  in the base plate decreases rapidly as a function of frequency. For the case where the thin-plate extensional wave speed of the constraining layer is less than that in the base plate, the third factor of Eq. (A1), considered as a function of  $c/c_3$ , has a minimum for  $c=c_3$ , equal to zero, and a maximum for  $(c/c_3)^2 = 1 + g'(1 + \beta^2)$ , equal to  $g'(1 + \beta^2)/(4 + \beta^2)$ . The minimum and maximum are very close together, since  $g'$  is small in this frequency range.

#### APPENDIX B: MODEL FOR EXTENSIONAL WAVES IN A FLUID-LOADED THIN PLATE

Thin-plate theory for flexural waves in a fluid-loaded plate may be found in Ref. 5. In that reference a term  $q$  is introduced into the equation for a beam<sup>9</sup> as a force per unit length and by analogy appears in the equation for a plate as a force per unit area, equal to the pressure of the fluid. This leads to the following wave equation for flexural waves in a fluid-loaded plate<sup>5</sup>

$$D\nabla^4 w + \rho_s h \frac{\partial^2 w}{\partial t^2} = -p|_{z=0}. \quad (\text{B1})$$

where  $\nabla^4$  is the biharmonic operator,  $D$  is the bending stiffness of the plate,  $D = (1/12)Eh^3/(1-\nu^2)$ ,  $E$  is Young's modulus,  $h$  is the plate thickness,  $\nu$  is Poisson's ratio,  $w$  is the displacement perpendicular to the plate,  $\rho_s$  the density of the plate material, and  $p$  the pressure in the fluid (fluid on one side). For two-sided fluid loading the pressure term is doubled.

The goal of the present derivation is to arrive at a similar equation for extensional waves in a thin, fluid-loaded plate, in the form

$$\frac{E}{(1-\nu^2)} \frac{\partial^2 w}{\partial x^2} + F = \rho_s \frac{\partial^2 w}{\partial t^2}, \quad (\text{B2})$$

where  $F$  is a fluid loading term, with the dimension of a force per unit length cubed. There was no indication found in the literature how this term could be related to the fluid pressure from first principles in the case of extensional waves, in contrast to flexural waves as shown in Eq. (B1).

Therefore, the problem was approached by means of thick-plate theory for extensional waves.<sup>4,10</sup> Thick plate theory carries the approximation implied by thin-plate theory to the next power of the dimensionless wave number  $kd$ , where  $k$  is the wave number and  $d$  the half-thickness of the plate. The result for flexural waves is known as Timoshenko-Mindlin plate theory.<sup>11</sup> In this type of theory the fluid loading appears naturally as a consequence of the introduction of the structural equations for the plate. Once the fluid-loading term has been introduced, thin-plate theory with fluid loading follows by taking the limit  $kd \rightarrow 0$ .

By integrating the differential equations of motion from exact elasticity theory or the corresponding momentum equations in the direction  $z$  perpendicular to the direction of propagation  $x$  (parallel to the faces of the plate), one obtains the following structural equations for extensional (symmetric) waves.<sup>10</sup>

$$(\lambda + 2G) \frac{\partial^2 U}{\partial x^2} + \lambda \frac{\partial \chi}{\partial x} + \rho_s \omega^2 U = 0 \quad (B3)$$

and

$$\frac{2}{3} d^2 \kappa^2 G \frac{\partial^2 \chi}{\partial x^2} - 2(\lambda + 2G) \chi - 2\lambda \frac{\partial U}{\partial x} + q^s + \frac{2}{3} \rho_s \omega^2 d^2 \chi = 0, \quad (B4)$$

where the displacement  $u$  in the direction of propagation  $x$  is given by a  $z$ -independent function  $U(x)$ , while the  $z$  displacement  $w$  is approximated by an antisymmetric linear expression in  $z$ ,  $w = z\chi(x)$ . Here  $\lambda$  and  $G$  are the Lamé constants,  $\omega$  is the angular frequency,  $d (= h/2)$  is the half-

thickness of the plate, and  $\kappa$  is a coefficient accounting for the varying shear in the plate. The fluid loading is represented by the term  $q^s$ ; the superscript  $s$  indicates extensional waves, for which  $q^s = \sigma_+ + \sigma_-$ , where  $\sigma_{\pm}$  are the normal stresses at the two faces of the plate, equal to the negative of the pressures on the faces.

Assuming a harmonic straight-crested wave with space and time dependence according to  $\exp i(\omega t - kx)$ , where  $k$  is the (complex) wave number,  $k = k' - i\alpha$ , one finds the dispersion relation by equating to zero the determinant of the matrix  $M_e$  of the coefficients of the amplitudes  $U, \chi$  in the two Eqs. (B3) and (B4)

$$M_e = \begin{bmatrix} -k^2(\lambda + 2G) + \rho_s \omega^2 & -ik\lambda \\ 2ik\lambda & -\frac{2}{3} d^2 \kappa^2 G - 2(\lambda + 2G) + \frac{2}{3} \rho_s \omega^2 d^2 + q^s/\chi \end{bmatrix} \quad (B5)$$

By manipulating the equation  $\text{Det}(M_e) = 0$ , one finds

$$\begin{vmatrix} (\lambda + 2G) - \rho_s c^2 & \lambda \\ \lambda & (\lambda + 2G) + \frac{1}{3} (kd)^2 \kappa^2 G - \frac{1}{3} \rho_s c^2 (kd)^2 - q^s/(2\chi) \end{vmatrix} = 0. \quad (B6)$$

The thin-plate model follows by dropping terms of order  $(kd)^2$ . By expanding the determinant one obtains

$$(\lambda + 2G)^2 - \rho_s c^2 (\lambda + 2G) - \lambda^2 - [(\lambda + 2G) - \rho_s c^2] q^s/(2\chi) = 0. \quad (B7)$$

If one divides this equation by  $(\lambda + 2G) = \rho_s c_d^2$  and applies  $(\lambda + 2G) - \lambda^2/(\lambda + 2G) = E/(1 - \nu^2)$ , there results the equation

$$E/(1 - \nu^2) - \rho_s c^2 - [1 - (c/c_d)^2] q^s/(2\chi) = 0, \quad (B8)$$

where  $c_d$  is the dilatational wave speed in the plate material.

To see how the fluid loading appears in the wave equation for  $\omega (= \chi d)$ , the  $z$  displacement of the plate surface at the positive side, one compares this expression with the proposed thin-plate equation with fluid loading Eq. (B2). Comparing Eqs. (B2) and (B8), one sees that the fluid-loading term  $F$  is given by

$$F = [1 - (c/c_d)^2] (kd)^2 q^s/(2d). \quad (B9)$$

The form of this equation suggests that it would be difficult to derive this expression from mechanical principles.

To obtain an equation in the variable  $k$  one uses Euler's equation. For fluid loading on both sides, one has  $q^s = 2\omega^2 \rho_0 \omega / (k^2 - k_0^2)^{1/2}$ , where  $\rho_0$  is the density of the medium and  $k_0$  the wave number in the medium. This expression is inserted into Eq. (B8). Similar to the development in Ref. 5, the resulting equation acquires a simple form if one introduces a new variable  $\tau$  defined by  $(k_0 \tau)^2 = k^2 - k_0^2$ . After some manipulation, the result is a third-degree equation in  $\tau$

$$\tau^3 - \Omega \tau^2 + \tau [1 - (c_0/c_p)^2] - \Omega [1 - (c_0/c_d)^2] = 0, \quad (B9)$$

where  $c_p$  is the wave speed for extensional waves in a thin plate. A characteristic frequency  $\omega_c$  and a dimensionless frequency  $\Omega$  are introduced by  $\omega_c = (\rho_s/\rho_0) c_p^2/(c_d d)$  and  $\Omega = \omega/\omega_c$ .

<sup>1</sup>E. M. Kerwin, "Damping of flexural waves by a constrained viscoelastic layer," *J. Acoust. Soc. Am.* **31**, 952-962 (1959).

<sup>2</sup>P. S. Dubbelday, "Constrained-layer model investigation based on exact elasticity theory," *J. Acoust. Soc. Am.* **80**, 1097-1102 (1986).

<sup>3</sup>P. S. Dubbelday and L. V. Fausett, "Constrained-layer damping analysis for flexural waves in infinite fluid-loaded plates," *J. Acoust. Soc. Am.* **90**, 1475-1487 (1991).

<sup>4</sup>P. S. Dubbelday, "Analysis of constrained-layer damping of flexural and extensional waves in infinite, fluid-loaded plates," in *Proceedings of the Second International Congress on Recent Developments in Air- and Structure-borne Sound and Vibration*, 4-6 March 1992, Auburn University, edited by M. J. Crocker and P. K. Raju (Mech. Eng. Dept., Auburn University, Auburn, AL, 1992), Vol. 1, pp. 151-156.

<sup>5</sup>M. C. Junger and D. Feit, *Sound, Structures, and Their Interaction* (MIT, Cambridge, 1986), 2nd ed., Secs. 8.1 and 8.2.

<sup>6</sup>I. A. Viktorov, *Rayleigh and Lamb Waves* (Plenum, New York, 1967).

<sup>7</sup>R. D. Mindlin, "An introduction to the mathematical theory of vibrations of elastic plates," Signal Corps Engineering Laboratories, Fort Monmouth, New Jersey (1955), Sec. 2.07.

<sup>8</sup>P. S. Dubbelday, "Investigation of constrained-layer technique using exact elasticity theory," in *Mathematical Modelling in Science and Technology*, Proceedings of the Fifth ICM, 29-31 July 1985, Univ. of California—Berkeley, edited by X. J. R. Avula, G. Leitmann, C. D. Mote, Jr., and E. Y. Rodin (Pergamon, New York, 1986), pp. 327-331.

<sup>9</sup>Reference 5, p. 199.

<sup>10</sup>P. S. Dubbelday, "Contribution of antisymmetric and symmetric waves to the reflection of sound in a fluid by a thick, homogeneous plate," NRL Memorandum Report 4312, Naval Research Laboratory, Orlando, FL (1980).

<sup>11</sup>Reference 5, Sec. 7.11.